Water Science & Technology

IWA PUBLISHING

Water Science & Technology Vol 87 No 1, 99 doi: 10.2166/wst.2022.393

Effect of Fe and Al based coagulants and disinfectants on polyethylene microplastics removal in coagulation process through response surface methodology

Fatemeh Tabatabaei[a], Roya Mafigholami[a,*], Hamid Moghimi[b] and Sanaz Khoramipoor[a]

[a] Faculty of Environmental Science and Engineering, Islamic Azad University, West Tehran Branch, Tehran, Iran
[b] Department of Microbiology, University of Tehran, Tehran, Iran
*Corresponding author. E-mail: r.mafigholami@wtiau.ac.ir

ABSTRACT

Microplastic (MP) pollution has been rising as a threatening risk and recently has appealed to the attention of more researchers. In this study, influential parameters affecting the removal rate of polyethylene microplastics (PEMPs) were optimized through response surface methodology (RSM). In Box Behnken Design (BBD), independent parameters were pH, PEMP size, coagulant dosage and polyacrylamide dosage. Two experimental sets were conducted, one with ferric chloride and the second with poly aluminum chloride as two commonly applied coagulants in drinking water treatment plants (DWTPs). Comparing the results of optimized parameters, PAC was a better coagulant with the predicted removal rate of 58.19%, while the removal rate with ferric chloride as a coagulant was predicted to be 56.37%. Moreover, some experiments were conducted to analyze the effect of ozone gas and sodium hypochlorite as disinfectants on removal rate. The highest removal rate was observed when 2 ppm of O_3 was added to the solution coagulated with optimal dosage of PAC, reaching the removal rate of 76.8%.

Key words: coagulation, disinfection, microplastics, polyethylene, RSM

HIGHLIGHTS

- Use of RSM for MPs removal optimization in coagulation process.
- Investigation of disinfectant effects on MPs sinking behavior.
- Comparison of two commonly used coagulants in optimization.
- Comparison of ozone and chlorine as disinfectants in MPs removal behavior.

INTRODUCTION

Recently, microplastics (plastic particles smaller than 5 mm in size; MPs) pollution has been considered a major problem worldwide due to its ubiquity, persistence and potential threat to living organisms (Schmidt *et al.* 2020; Shruti *et al.* 2020; Qiang & Cheng 2021). Among the polymer types of plastics, polypropylene (PP; 19.7%), low-density polyethylene (LDPE; 17.4%) and high-density polyethylene (HDPE; 12.9%) comprise the most produced plastic material (PlasticEurope 2021). There are two types of MPs in terms of origination: Primary MPs that are directly manufactured for consumer or industrial purposes including personal care products (Jaikumar *et al.* 2019), exfoliating products (Adib *et al.* 2021) and air-blasting technology (Wu *et al.* 2016) and secondary MPs that originate from the fragmentation of larger plastic materials through weathering (Anderson *et al.* 2017), laundering (Raju *et al.* 2018), photodegradation (Hebner & Maurer-Jones 2020) and biological degradation (Sighicelli *et al.* 2018). Since these particles are not completely removed in wastewater treatment plants (Kay *et al.* 2018; Prata 2018; Magni *et al.* 2019) (WWTPs), they end up in freshwater resources through effluent release to the environment along with deposition of airborne MPs (Klein & Fischer 2019; Wright *et al.* 2020) and people activities (Schmidt *et al.* 2020). Hence, a significant amount of MPs has been detected in rivers (Lin *et al.* 2018; Crew *et al.* 2020) and lakes (Grbić *et al.* 2020; Mao *et al.* 2020a).

Generally, drinking water treatment plants (DWTPs) feed from freshwater resources to provide drinking water to people. However, these facilities are not also able to completely remove MPs, thereby a significant number of MPs have been observed in treated water (Pivokonsky *et al.* 2018; Pivokonský *et al.* 2020; Wang *et al.* 2020b; Adib *et al.* 2021). For example,

Tong *et al.* (2020), according to their results from MP pollution in tap water in China, reported that adult individuals are prone to intake 660 MPs per day (Tong *et al.* 2020). Not only do MPs cause adverse effects on humans when ingested (Hwang *et al.* 2020; Çobanoğlu *et al.* 2021; Zhang *et al.* 2022), they are able to adsorb other pollutants in the natural environment and desorb them in the body (Llorca *et al.* 2020; Zhou *et al.* 2020; You *et al.* 2021). Based on the identification of MPs in treated water in DWTPs, multiple shapes include fibers, fragments, spheres and films, but in terms of MP size, particles down to the size of one μm have been investigated (Pivokonsky *et al.* 2018; Pivokonský *et al.* 2020; Wang *et al.* 2020b; Adib *et al.* 2021). In DWTPs, the coagulation/flocculation process has a great role in the removal of MPs (Tang & Hadibarata 2021), but the removal rate in this process differs based on multiple factors including coagulant type and dosage. In some studies, it is observed that the removal rate is as low as 48.4% (Adib *et al.* 2021) to as high as 88.6% (Wang *et al.* 2020b). Therefore, removal characteristics of MPs in DWTPs should be further investigated.

Iron and aluminum salts are commonly used as coagulants in the coagulation/flocculation process (Jiang 2015). Therefore, these materials were mostly investigated in MP removal characterization by the coagulation process (Ma *et al.* 2019a, 2019b; Lu *et al.* 2021; Xue *et al.* 2021). For example, Ma *et al.* (2019a) investigated the removal characteristics of pristine PE MPs by ferric chloride and they observed that 90.91 $\pm$ 1.01% of PE MPs were removed by 2 mM (540 mg/L) ferric chloride coupled with 15 mg/L polyacrylamide (Sarmah & Rout 2018) as coagulants. Moreover, Zhang *et al.* (2021b) reached a removal rate of 91.45% for Polyethylene Terephthalate (PET) MPs with 200 mg/L polyaluminum chloride (Paço *et al.* 2017) and 100 mg/L PAM. According to the typical coagulant dosage in DWTPs, the amount of coagulants for MP removal in the mentioned studies is very high. However, in some other studies, lower amounts of coagulants with desirable results have been observed (Li *et al.* 2021; Xue *et al.* 2021). It is worth mentioning that the removal characterization of pristine and weathered MPs differ due to variation in density, changes in chemical bonds and adsorption of different materials on the surface of MPs (Monira *et al.* 2021; Nakazawa *et al.* 2021). Since MPs in nature are weathered, it is not suggested to utilize pristine MPs in removal characterization. In addition, it has been observed that chlorination and ozonation can affect the chemical properties of MPs (Kelkar *et al.* 2019; Li *et al.* 2022) which can influence the sinking speed of these particles (Lin *et al.* 2022). However, to the best knowledge of the authors, no studies have investigated the effect of both coagulation and disinfection on the MP removal rate. Therefore, this study aims to compare the use of ferric chloride and PAC as coagulants to remove MPs through Response Surface Methodology (RSM). In this regard, four variables including pH, PEMPs size, coagulant and PAM concentration will be evaluated. Afterward, the influence of chlorination and ozonation process on MP removal after the coagulation will also be investigated.

MATERIALS AND METHODS

Materials

All the chemicals used in this study were analytical grade from Merck, Germany, unless stated, including sodium hydroxide (NaOH), hydrochloric acid (HCl), kaolin, sodium chloride (NaCl), humic acid (HA; Sigma Aldrich, USA), ferric chloride ($FeCl_3$). PAC was purchased from Tianshi (Jiangsu) Fine Chemicals Co. (Changzhou, China) and sodium hypochlorite (NaOCl) was provided from Neutron Chemical Company (Tehran, Iran). All the samples were conducted with prefiltered deionized water. Polyethylene microplastics (PEMPs) were provided by milling PE pellets (0.92 $g{\cdot}cm^{-3}$, LL 0209 KJ, Shazand Petrochemical company, Iran) by an ultra-centrifugal mill (ZM 200, Retsch®, Germany) until they were micronized. The composition of purchased pellets was characterized by Fourier Transform Infrared Spectrophotometer (FT-IR; Avatar 380, Thermo Scientific, USA). Data acquisition was conducted in the transmission mode of 2 cm^{-1} resolution, and collection time of 3 s, wavenumber ranging from 400 to 4000 cm^{-1}. Spectra were compared with a database provided by Omnic software (Thermo Phisher Scientific, USA). Before milling, the pellets were immersed in liquid nitrogen until they reached −196 °C. Finally, PEMPs were sieved into two different sizes, including $40 < d < 70$ μm and $70 < d < 100$ μm. Moreover, clear PE microspheres with the size of $10 < d < 45$ μm were provided from Cospheric, CA, USA.

Coagulation experiment

First, to remove residuals, PEMPs were immersed in 1 M HCl and were placed in oven at 70 °C for 24 h until they were fully dried. As described by Ma *et al.* (2019a, 2019b) and Adib *et al.* (2022), 0.5 L beakers were used to carry out the experiments (Ma *et al.* 2019b; Adib *et al.* 2022). To simulate turbidity, kaolin was added to DI water until it reached to 5 NTU by a turbidity meter (AL450T-IR, Aqualytic, Germany). Five NTU is the average turbidity of DWTPs of Iran (Hashempour & Mortezazadeh 2020). Moreover, background ionic strength was created by adding 0.1 M NaCl to the solution (Wang *et al.* 2013) and natural

organic matter (NOM) was simulated by adding 1 mg/L HA to the solution. Then, to adjust pH, a prepared 1 M HCl and 1 M NaOH solution was used and the pH of stock solution was measured by a pH meter (3510, Jenway, UK). Afterward, 0.100 g of PEMPs were added to the solution. All the chemicals used in the solution were balanced by precision balance with a minimum range of 1.0×10^{-3} g (LST-JM-102, CGOLDENWALL, China). Finally, a predetermined amount of coagulant (whether PAC or ferric chloride) and anionic PAM were added to the solution 30 s after the start of mixing by a Jar test apparatus (Tak Azama, Iran). The solution was mixed for 1 min at 300 rpm, following a slow stirring of 14 min at 100 rpm (Ma *et al.* 2019a, 2019b; Monira *et al.* 2021; Zhang *et al.* 2021b; Adib *et al.* 2022). After the stirring, samples were left for 30 min for sedimentation (Sillanpää *et al.* 2018). In this study, to measure the removed PEMPs, a weighing method was used (Ma *et al.* 2019b; Adib *et al.* 2022). In this method, supernatants were carefully removed from the beaker and filtered through a 0.45 μm membrane filter. To digest the flocs, supernatants on the filter were immersed in 1 M HCl for 1 h and treated in an ultrasonic bath for 5 min. Then, the supernatants were filtered again and dried in an oven at 70 °C for 12 h. After drying, according to Equation (1), the weight of the removed PEMPs based on percentage was calculated (W_{dried}):

$$PEMPs\ removal = \frac{W_{total} - W_{dried}}{W_{total}} \times 100 \quad (1)$$

Aside from the characterization of PEMPs, a mixture of these particles trapped in the flocs made by coagulants, with or without PAM was also characterized by FT-IR analysis. Moreover, electro-kinetic potential of the solution in three different pH was also measured by a zeta potential analyzer with a measurement range of ± 200 mV (SZ-100, Horiba Scientific, Japan). Furthermore, the dynamic size of the formed flocs (d_{50}) in three pH ranges were measured every 30 s by a static light scattering (SLS) particle size analyzer (PSA) with particle size range of 0.02–2000 mm (SLS-PSA; Mastersizer 2000, Malvern panalytical, UK). Finally, morphology of the PEMPs was analyzed using a scanning electron microscope (Quanta 200, FEI ESEM, USA) equipped with Energy Dispersive X-ray Spectroscopy (EDX). The acceleration of SEM images was 25 kV and working distance (WD) of 9.6 mm. Before imaging, a gold layer was sputtered onto the samples to create conductivity. To prepare samples for SEM analysis, PAC or ferric chloride flocs trapping PEMPs, with or without PAM, were extracted from the bottom of the beaker and filtered through a membrane filter and dried for 12 h at 70 °C in an oven.

Experimental design

To optimize the parameters and to reach the highest rate of removal, RSM with Box Behnken Design (BBD) was utilized in this study. pH, coagulant dosage, PAM dosage and PEMPs size were chosen as independent variables and the removal rate was chosen as a dependent variable. As per the BBD model, three levels for each parameter were chosen in Design-Expert® software (Version 11, Stat-Ease Inc., USA); 5, 7 and 9 for pH, 6, 12 and 8 ppm for PAM dosage, 50, 200 and 350 ppm for coagulant dosage and 10–45, 40–70 and 70–100 μm for PEMP size (see Table 1; the data of this table were used for both PAC and ferric chloride coagulants).

According to Equation (2) (Parsa *et al.* 2020), 29 experiments were provided by Design-Expert including five replicated center points:

$$N = 2^k + 2k + N_0 = 16 + 8 + 5 = 29 \quad (2)$$

where N is the number of total experiments, k is the number of independent variables and N_0 is the replicated center points. In this equation, 2_k and $2k$ represent factorial points and axial points, respectively. Table 2 represents the 29 experiments with PAC and ferric chloride in different conditions. In total, 58 experiments were conducted with both coagulants.

Table 1 | Three levels of chosen independent variables designed by BBD model

Factor	Unit	Low	Middle	High
PEMP size	μm	10 (10–45)	40 (40–70)	70 (70–100)
pH	–	5	7	9
Coagulant dosage	ppm	50	200	350
PAM dosage	ppm	6	12	18

Table 2 | Actual and predicted values of removal rate with ferric chloride and PAC at different conditions

Std	A:pH –	B:PEMP size mm	C:Coagulant concentration ppm	D:PAM concentration ppm	MP removal (PAC		MP removal (ferric chloride)	
					Actual	Predicted	Actual	Predicted
					%			
1	5	10	200	12	0.5	0.39	18.7	15.79
2	9	10	200	12	24.7	22.72	55.3	47.59
3	5	70	200	12	14.7	16.68	16.2	15.54
4	9	70	200	12	43.9	39.02	32.8	27.34
5	7	40	50	6	38.2	40.46	36.1	29.09
6	7	40	350	6	7.8	8.76	12.8	11.64
7	7	40	50	18	10.9	12.73	18.7	26.39
8	7	40	350	18	36.5	37.03	11.5	8.94
9	5	40	200	6	2.3	6.75	8.5	9.47
10	9	40	200	6	59.1	52.78	25.9	31.27
11	5	40	200	18	20.8	30.71	6.8	6.77
12	9	40	200	18	30.2	29.35	24.9	28.57
13	7	10	50	12	13.5	8.25	34.7	40.41
14	7	70	50	12	23.9	24.55	28.2	30.16
15	7	10	350	12	4.7	4.55	22.8	22.96
16	7	70	350	12	19.5	20.85	12.2	12.71
17	5	40	50	12	10.9	3.98	26.6	24.39
18	9	40	50	12	18.9	26.32	44.5	46.19
19	5	40	350	12	9.6	0.29	0.3	6.94
20	9	40	350	12	16	22.62	24.5	28.74
21	7	10	200	6	19.2	22.86	22.5	25.49
22	7	70	200	6	33.6	39.16	16.4	15.24
23	7	10	200	18	19.3	23.13	28.7	22.79
24	7	70	200	18	44.1	39.43	15.4	12.54
25	7	40	200	12	45.2	41.34	29.8	26.56
26	7	40	200	12	41.6	41.34	30.7	26.56
27	7	40	200	12	44.8	41.34	25.3	26.56
28	7	40	200	12	45.8	41.34	26.2	26.56
29	7	40	200	12	39.9	41.34	22.8	26.56

In total, 29 experiments with ferric chloride and 29 experiments with PAC were conducted.

Based on the fit summary, a quadratic model (p-value < 0.00001) was suggested. In this model, AB, AC, BC, BD and D^2 for PAC experiments and AC, AD, BC, BD, CD, A^2, B^2 and C^2 were omitted from analysis of variance (ANOVA), since they were not significant (p-value > 0.1). Moreover, Equation (3) (Parsa *et al.* 2020) was used as a relationship between independent and dependent variables:

$$Y = \beta_0 + \sum_{i=1}^{k} \beta_i x_i + \sum_{i=1}^{k} \beta_i x_i^2 + \sum_{i=1}^{k} \sum_{j=1}^{k} \beta_i x_i x_j \quad (3)$$

where Y is predicted response (removal rate), β_0 is the constant regression coefficient for the intercept, β_i is the linear coefficient, β_{ii} is the quadratic coefficient, β_{ij} is the interaction coefficient, x_i and x_j are coded values for independent variables.

Using Design-Expert® coefficient (R^2_{adj}), standard software, analysis of variance (ANOVA) and regression coefficients were applied to analyze data at the 90% confidence level. Multiple factors of practical data sets were analyzed to test the model fitness, including F-value, *p*-value, degree of freedom (DF), mean square (MS), sum of squares (SS), correlation coefficient (R), determination coefficient (R^2), adjusted R^2, standard deviation and coefficient of variance (CV).

Disinfection experiments

After achieving the optimum points in all four parameters, other experiments were conducted by adding ozone gas (O_3) or sodium hypochlorite (NaOCl, 6–14% active chlorine) as disinfectants to simulate disinfection unit of a DWTP. When stirring with the Jar test was finished, the solution was instantly decanted into an Imhoff cone equipped with a glass faucet. Three levels of concentration (1, 2 and 3 mg/L) for O_3 or NaOCl (with PAC or ferric chloride) were considered to evaluate the rate of removal at disinfection unit. The O_3 gas was generated by an ozone generator with a capacity of 3 g/h. O_3 gas was transferred through a plastic hose capped with a rectangular ozone diffuser. Thirty min after sedimentation, O_3 or NaOCl were added to the solution and after another 30 min, the faucet was opened to release the settled floc until supernatants remained. Finally, supernatants were collected and immersed in 1 M HCl for flocs containing PEMPs to be digested. Then, PEMPs were filtered and dried in an oven at 70 °C for 12 h.

RESULTS AND DISCUSSION

Statistical analysis

To predict the removal rate (response value) in different situations, independent variables (A: pH, B: PEMP size, C: coagulant concentration and D: PAM concentration) were applied in Equations (4) and (5) based on ferric chloride and PAC, respectively:

$$Y = 26.56 + 10.9A - 5.13B - 8.73C - 1.35D - 5AB - 7.55D^2 \quad (4)$$

$$Y = 41.34 + 11.17A + 8.15B - 1.85C + 0.13D - 11.85AD + 14CD - 11.45A^2 - 10.2B^2 - 16.6C^2 \quad (5)$$

where Y is the response value (removal rate), AB, AD and CD are interaction effects and A^2, B^2, C^2 and D^2 are two second-order effects for A, B, C and D, respectively. Table 3 represents analysis of variance (ANOVA) for both responses. All the coefficient variables were evaluated at 95% confidence level. In this table, F-value shows the effectiveness of the variable which was 25.27 and 22.61 for ferric chloride and PAC, respectively. Other evaluated data sets are DF, MS, *p*-value, coefficient of variance (CV) for checking fitness of the model, standard deviation, R^2 and adjusted R^2 (Singh & Kumar 2020).

In the chosen model, based on ANOVA, R^2 and the adjusted R^2 are 0.87 and 0.84 for ferric chloride and 0.92 and 0.87 for PAC, respectively. Generally, higher R^2 represents a close relation between actual and predicted value. Moreover, a higher F-value indicates that the variable has more impact on the coagulation process.

Effect of coagulant concentration on PEMP removal

The concentration of ferric chloride and PAC (50, 200 and 350 ppm) were investigated along with different conditions of other variables. It is clear that by the increase of coagulant dosage, the removal rate did not increase, rather it was observed that nearly no flocs were created in most of the experiments with 350 ppm ferric chloride or PAC and the turbidity of water increased due to the presence of dissolved coagulants, because in lower turbidity, a higher amount of coagulant is not effective to create flocs (Rawi *et al.* 2014). Therefore, lower amounts of coagulants (less than 200 ppm) were more effective in removal rate. However, based on the BBD model, the optimum concentration of ferric chloride was chosen at the minimum value (50 ppm) and that of PAC was chosen at 128 ppm. This suggests that the optimum concentration of ferric chloride can be found even lower than 50 ppm, but due to the range of investigated concentration, the minimum amount was suggested by the model. Moreover, the effectiveness of the variable in removal rate (F-value) for ferric chloride was 43.6 and for PAC was 1.32. This indicates that ferric chloride was the second most influential variable among other variables, while the effectiveness of PAC along with the other two variables (pH and PEMP size) was less significant. In other similar studies, it has been observed that usage of 2 mM (324 ppm) ferric chloride coupled with PAM removed more than 90% of PEMP of smaller than 500 μm (Ma *et al.* 2019a). Unlike the present study, they did not face any decrease in removal rate by increasing the coagulant dosage from 1 to 5 mM (270 to 1351 ppm). This can be due to the fact that turbidity was constant in this study. Moreover, Xue *et al.* (2021), investigated the removal of carboxylated polystyrene microplastics (PSMPs) by alum-based coagulant (10–50 ppm). They observed that by increasing the coagulant dosage, the removal rate of larger particles improved,

Table 3 | Table of ANOVA for the quadratic model for PEMPs removal with ferric chloride and PAC

Source	Sum of squares	df	Mean square	F-value	*p*-value
Ferric Chloride					
Model	3177.06	6	529.51	25.27	<0.0001
A-pH	1425.72	1	1425.72	68.04	<0.0001
B-MP Size	315.19	1	315.19	15.04	0.0008
C-Coagulant Concentration	913.51	1	913.51	43.60	<0.0001
D-PAM Concentration	21.87	1	21.87	1.04	0.3181
AB	100.00	1	100.00	4.77	0.0399
D^2	400.77	1	400.77	19.13	0.0002
Residual	460.97	22	20.95		
Lack of Fit	418.28	18	23.24	2.18	0.2354
Pure Error	42.69	4	10.67		
Cor Total	3638.03	28			
SD = 4.58, C.V. = 19.53%, $R^2 = 0.8733$, $R^2_{adj} = 0.8387$					
PAC					
Model	6351.80	9	705.76	22.61	<0.0001
A-pH	1496.33	1	1496.33	47.94	<0.0001
B-MP Size	797.07	1	797.07	25.54	<0.0001
C-Coagulant Concentration	41.07	1	41.07	1.32	0.2656
D-PAM Concentration	0.2133	1	0.2133	0.0068	0.9350
AD	561.69	1	561.69	17.99	0.0004
CD	784.00	1	784.00	25.12	<0.0001
A^2	881.34	1	881.34	28.24	<0.0001
B^2	699.35	1	699.35	22.41	0.0001
C^2	1852.86	1	1852.86	59.36	<0.0001
Residual	593.07	19	31.21		
Lack of Fit	566.63	15	37.78	5.72	0.0522
Pure Error	26.43	4	6.61		
Cor Total	6944.87	28			
SD = 5.59, C.V. = 21.89, $R^2 = 0.9146$, $R^2_{adj} = 0.8742$					

while similar to this study, the removal rate of smaller particles did not improve when the dosage of coagulant was more than 30 ppm. They also speculated that turbidity of water influenced removal rate (Xue *et al.* 2021). Furthermore, Zhou *et al.* (2021) investigated the removal rate of PSMPs and PEMPs by ferric chloride and PAC and, similar to this study, they observed that PAC caused better results in removal rate (Zhou *et al.* 2021). In their study, different concentrations of coagulants, from 0 to 180 ppm, were examined. They observed that when PAC was 90 ppm, the removal efficiency of PEMPs was 29.7%, while with the increase in coagulant dosage, the removal rate either decreased or did not change. In a recent study, Adib *et al.* (2022) studied the removal of PPMPs in the coagulation process by PAC and anionic PAM. Due to the low density of PEMPs, they reached only 18.75% removal with PAC concentration of 200 ppm. This amount of PAC was at the minimum of the chosen range, which indicates that the chosen range in this study (50–350 ppm) was properly chosen. Figure 1 shows the morphology of PEMPs and PEMPs trapped in flocs (circled in yellow). EDX results of the following SEM images are also provided. From the surface of PEMPs, it is clear that the surface of PEMPs is rough and wrinkled which indicates that they were fairly aged (Mao *et al.* 2020b). Since PEMPs were kept in the laboratory for almost a year under room temperature and limited source of lamp light and the fact that they were able to adsorb HA (as a model of NOM), PEMPs are not considered virgin in this study.

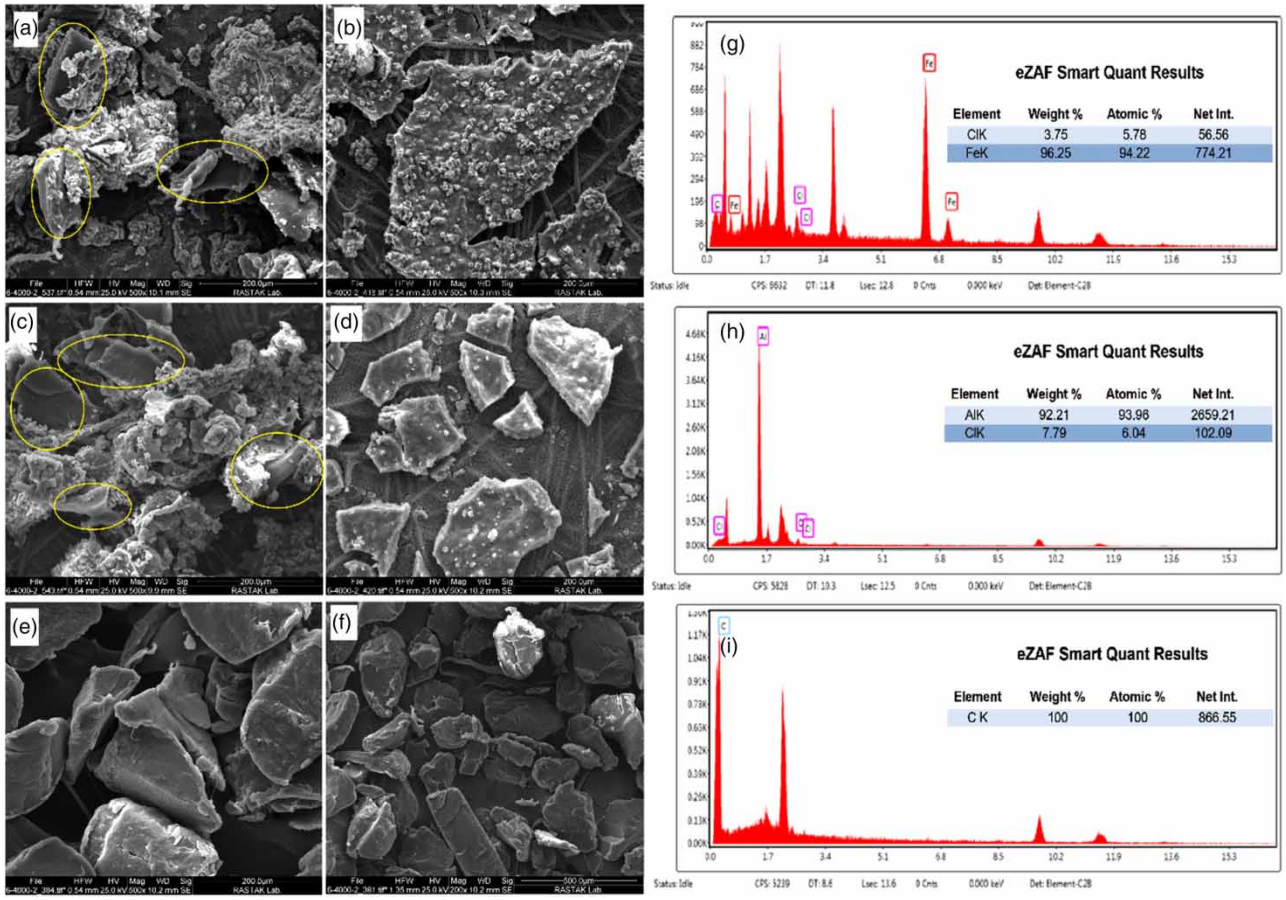

Figure 1 | SEM images: (a) PEMPs trapped in ferric chloride flocs, (b) flocs of ferric chloride without PEMPs, (c) PEMPs trapped in PAC flocs, (d) PAC flocs without PEMPs, (e) and (f) illustrate morphology of PEMPs before coagulation, (g) EDX result of ferric chloride flocs, (h) EDX result of PAC flocs and (i) EDX result of PEMPs.

Effect of pH on PEMP removal

Based on the BBD model, pH 5, 7 and 9 were studied in this process. In all the experiments, both in ferric chloride and PAC experiments, it has been observed that with the increase of pH, the removal rate of PEMPs increased. The effectiveness of this variable was highest among other variables in both PAC (F-value = 47.94) and ferric chloride (F-value = 68.04) experiments. According to the PSA results (Figure 2), with the increase in pH, the size of created flocs increased. Therefore, more PEMPs can be trapped into the flocs and settle due to the heavier agglomerated mass. Accordingly, the optimum level of pH was detected at the highest level of analyzed range (pH = 9). Based on Figure 2, mean floc size at pH 9 reached over 800 μm after 5 min, while it remained under 600 and 400 μm at pH 7 and 5, respectively. Moreover, it was clear that mean floc size did not change dramatically after 5 min, so the analysis of PAS stopped at 10 min. In a similar study, Ma *et al.* (2019a), by analyzing PSA results of floc size at same three pHs, observed that ferric chloride floc sizes were approximately 400, 600 and near 800 μm at pH 6, 7 and 8 (Ma *et al.* 2019a, 2019b). However, they continued the experiment with PSA until 15 min, but the floc size remained almost constant. In contrary to this study, Esfandiari & Mowla (2021) observed that a better removal rate of PEMPs happens at lower pH (Esfandiari & Mowla 2021). They analyzed the removal rate of PEMPs by coagulation and dissolved air flotation (DAF) at three pHs of (6, 7 and 8) through RSM. Although similar to this study, the removal rate at pH 6 with $AlCl_36H_2O$ was 59.5% which is very close to the result of the present study.

According to the zeta potential analysis (Figure 3), by the increase of pH, zeta potential decreased which means that particles tend to be less stable in comparison with lower pH. This supports the prediction of RSM in the BBD model that higher pH causes more removal of PEMPs. In this analysis, the zeta potential at pH 5 was 11.2 ± 1.3 mV, but the increase of pH to 7 and 9, the zeta potential reduced to 8.1 ± 1.2 and 4.6 ± 0.9 mV, respectively. However, at pH 10,

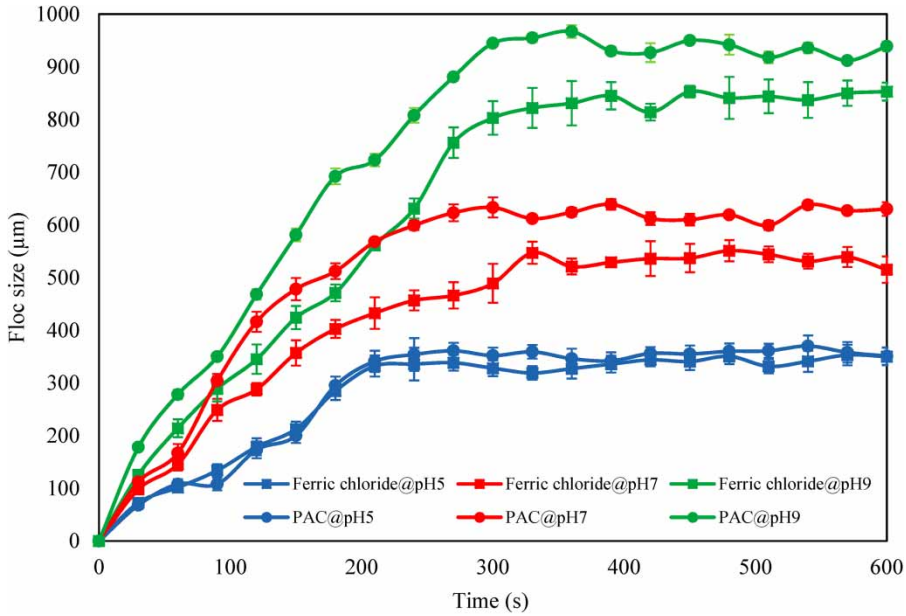

Figure 2 | Created floc size (d_{50}) based on time detected by PSA at three different pHs.

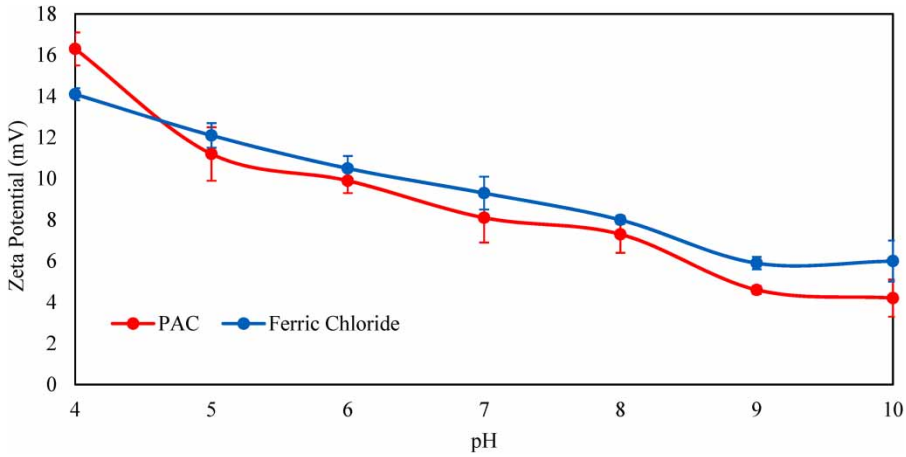

Figure 3 | Zeta potential of flocs created by ferric chloride (in red) and PAC (in blue) at different pH.

the zeta potential faced a negligible change which indicated that the removal rate does not appear to increase above pH 10.

In a study by Zhang *et al.* (2021a), coagulation removal of PEMPs in wastewater were analyzed via magnetic magnesium hydroxide coagulant (MMHC) and PAM as coagulants. In zeta potential analysis, they observed that zeta potential increased from −18 mV to −10 mV when pH increased from 7 to 9 which indicates that coagulant and kaolin interact with each other to form flocs (Zhang *et al.* 2021a). Similarly, Adib *et al.* (2022) analyzed zeta potential results in different pH. They similarly found out that by the increase of pH from 5 to 9, zeta potential decreased from 11.35 ± 0.15 to 3.85 ± 0.15%, approaching zero (Adib *et al.* 2022). This is in line with the results of this study, since zeta potential near zero means instability of particles and their inclination toward settling (Selvamani 2019). Moreover, Lu *et al.* (2021) faced a different result. They tested zeta potential at different concentrations of Al^{3+} as coagulant under pH 6, 7 and 8. They reported that dosage of coagulant was significant in the removal of PET-MPs, while the solution pH was not (Lu *et al.* 2021). They reckoned that discordant results in zeta potential is due to the various types of MPs analyzed and different conditions of mixing solution in the Jar test.

Effect of PEMP size on PEMP removal

Three size ranges of PEMPs including 10–45, 40–70 and 70–100 μm were studied in this process. This variable was the third influential parameter in the ferric chloride experiment (F-value = 15.04), but with F-value = 25.54, the effectiveness was the second among the other three variables. In the experiment with ferric chloride, the optimum particle size was detected at the minimum of the analyzed range (10 μm: 10–45 μm), while the optimum size in PAC experiments was 52 μm: 40–70 μm. This can be due to the smaller dynamic size of the flocs created by ferric chloride, since larger flocs are capable of trapping larger MPs. Figure 4 is the result of characterization of PEMPs with coagulants by FTIR. In combination with PEMPs + ferric chloride and PEMPs + ferric chloride + PAM, Alcohol/Phenol O-H Stretch (3200–3550 cm^{-1}) is more pronounced than other spectra. Moreover, Alkyl C-H Stretch (2850–2950 cm^{-1}) is stronger in PEMPs spectrum than its combination with coagulants. Furthermore, Aromatic C = C Bending (1500–1700 cm^{-1}) became stronger in PEMPs and coagulants than PEMPs alone. However, 721 cm^{-1} (rocking deformation) and 1468 cm^{-1} (bending deformation) in PEMPs decreased in strength in combined coagulant spectra.

Figure 5 illustrates diagrams related to the result of optimum condition with ferric chloride. Figure 5(a) and 5(b) show 3D and 2D diagrams of pH and PEMPs size interaction. It is clear that with the decrease in PEMPs size, the removal rate increases. Figure 5(d) shows that PEMPs size and pH influence on removal rate is linear. In different studies that investigated coagulation removal of MPs, the size of these particles has been influential in the sinking behavior of flocs. For example, Xue *et al.* (2021) used 6, 25, 45 and 90 μm PS microspheres in coagulation-flocculation sedimentation (CFS) treatment. They reported that the removal of MPs decreased with an increase in their size (Xue *et al.* 2021). Similarly, Adib *et al.* (2022) and Ma *et al.* (2019a) reported that smaller PEMPs can be easily removed in comparison with larger particles (Ma *et al.* 2019b; Adib *et al.* 2022). However, Zhang *et al.* (2021b) investigated the coagulation of coagulation characteristics of PET-MPs and observed that larger MPs with the size of 400–500 μm were removed better than smaller PET-MPs with the size of 100–400 and smaller than 100 μm (Zhang *et al.* 2021b). This difference in results can be ascribed to the polymer type of MPs.

Effect of PAM concentration on PEMP removal

PAM is a coagulant-aid that is usually added to water coupled with coagulants to boost the sedimentation rate of suspended particles (Xiong *et al.* 2018). In this study, this variable had the least efficacy in both ferric chloride (F-value = 1.04) and PAC (F-value = 0.007) experiments. The optimum dosage of PAM in ferric chloride experiments was detected at 11.4 ppm, but with PAC experiments it was the minimum of the analyzed range (6 ppm). Figure 5 represents diagrams of coagulation experiments with PAC. Figure 5(a) shows a 3D diagram of interaction between PAM dosage and pH. With the decrease in PAM dosage, it is clear that removal rate decreases too. However, excess in using PAM did not have a direct relationship with removing PEMPs and the removal rate remained almost constant. This effect has been observed in other studies too

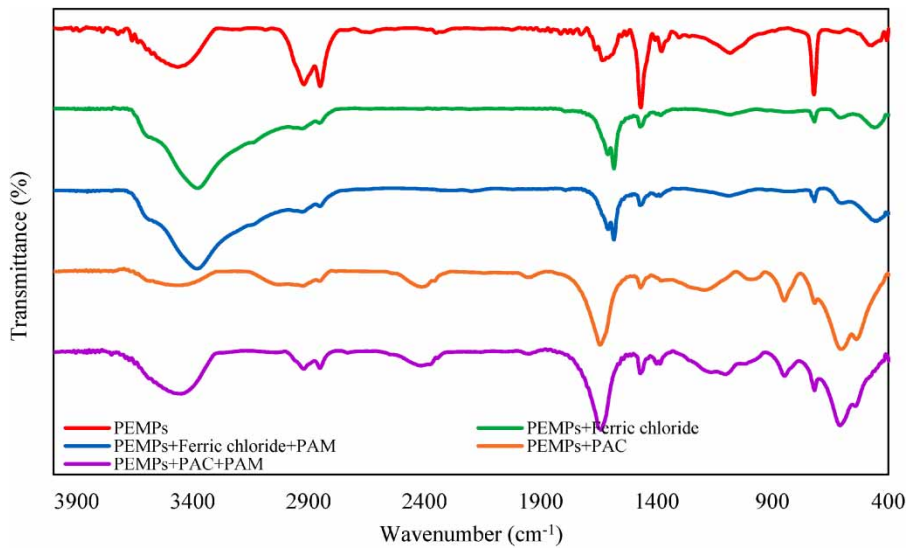

Figure 4 | FTIR analysis of PEMPs and PEMPs trapped in flocs of PAC or ferric chloride with the presence or absence of PAM.

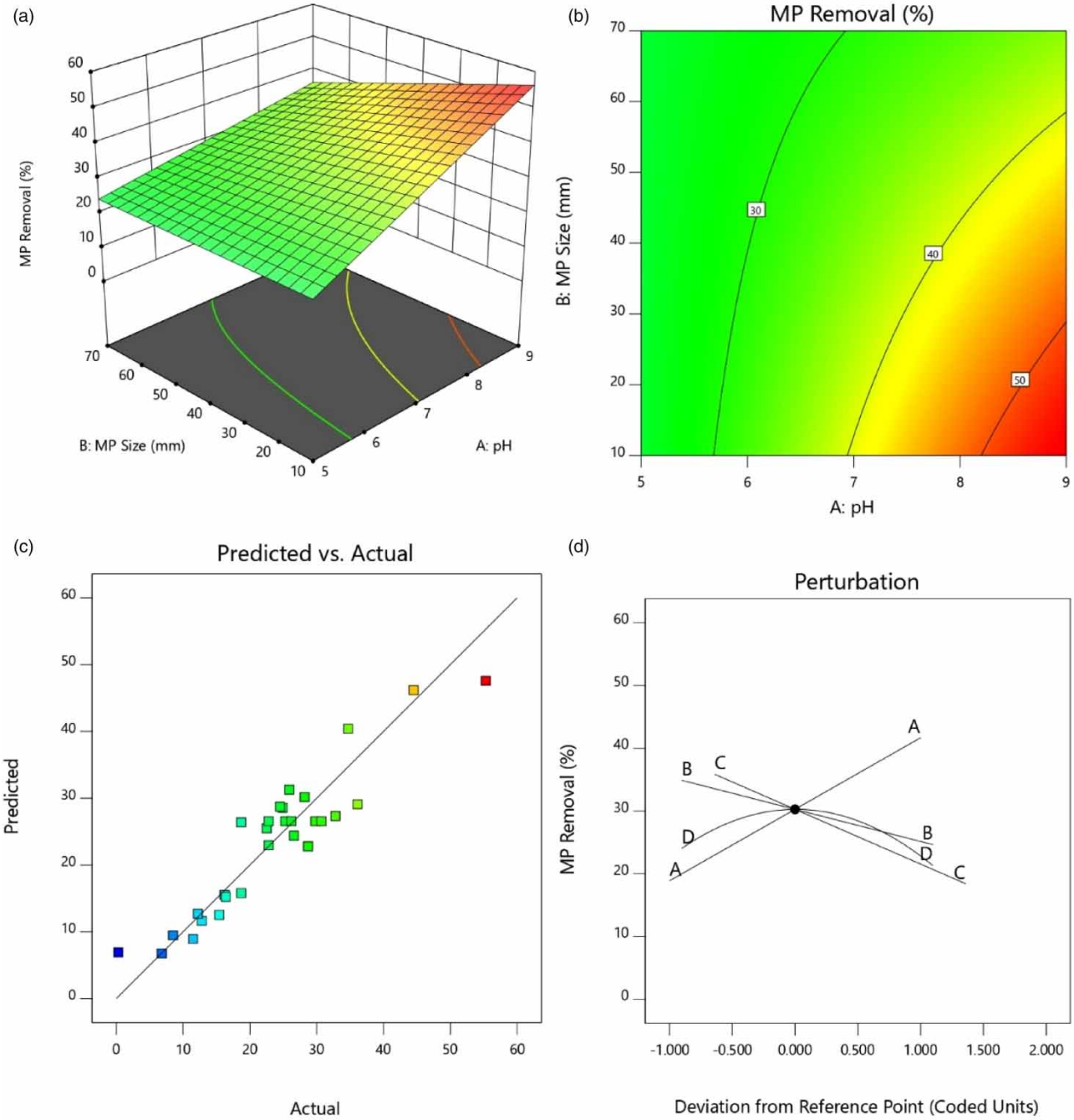

Figure 5 | Diagrams of optimum condition with ferric chloride in which (a) shows 3-D diagram of interaction between pH and PEMP size, (b) illustrates 2-D diagram of pH and PEMP size interaction, (c) illustrates comparison of 29 actual and predicted experiments and (d) shows perturbation plot of four analyzed variables.

(Ahmad *et al.* 2008; Kim 2016; Liu *et al.* 2017). For example, Ma *et al.* (2019b) observed that usage of PAM increased the removal rate of small PEMPs (smaller than 0.5 mm), but the highest removal rate with anionic PAM was at 3 ppm and for cationic PAM was 6 ppm. More usage of PAM decreased the removal rate (Ma *et al.* 2019b). However, Zhang *et al.* (2021a) changed the value of PAM in the presence of a constant amount of mg$(OH)_2$ and F_3O_4 to remove virgin PEMPs smaller than 270 μm. They reported that with the increase in PAM dosage, removal rate increased, but they stopped the test at 5 ppm of PAM (Zhang *et al.* 2021a).

Optimization

Based on the BBD model in Design-Expert software, variables were optimized to reach the maximum removal rate of PEMPs. In this regard, based on Figure 6, in the experiments with ferric chloride as a coagulant, the optimum condition of variables were pH 9, PEMP size 10 μm (10–45 μm), ferric chloride dosage of 50 ppm and PAM dosage of 11.4 ppm. With the mentioned conditions, maximum removal rate was predicted to be 56.4% which was acquired by setting the variables 'In

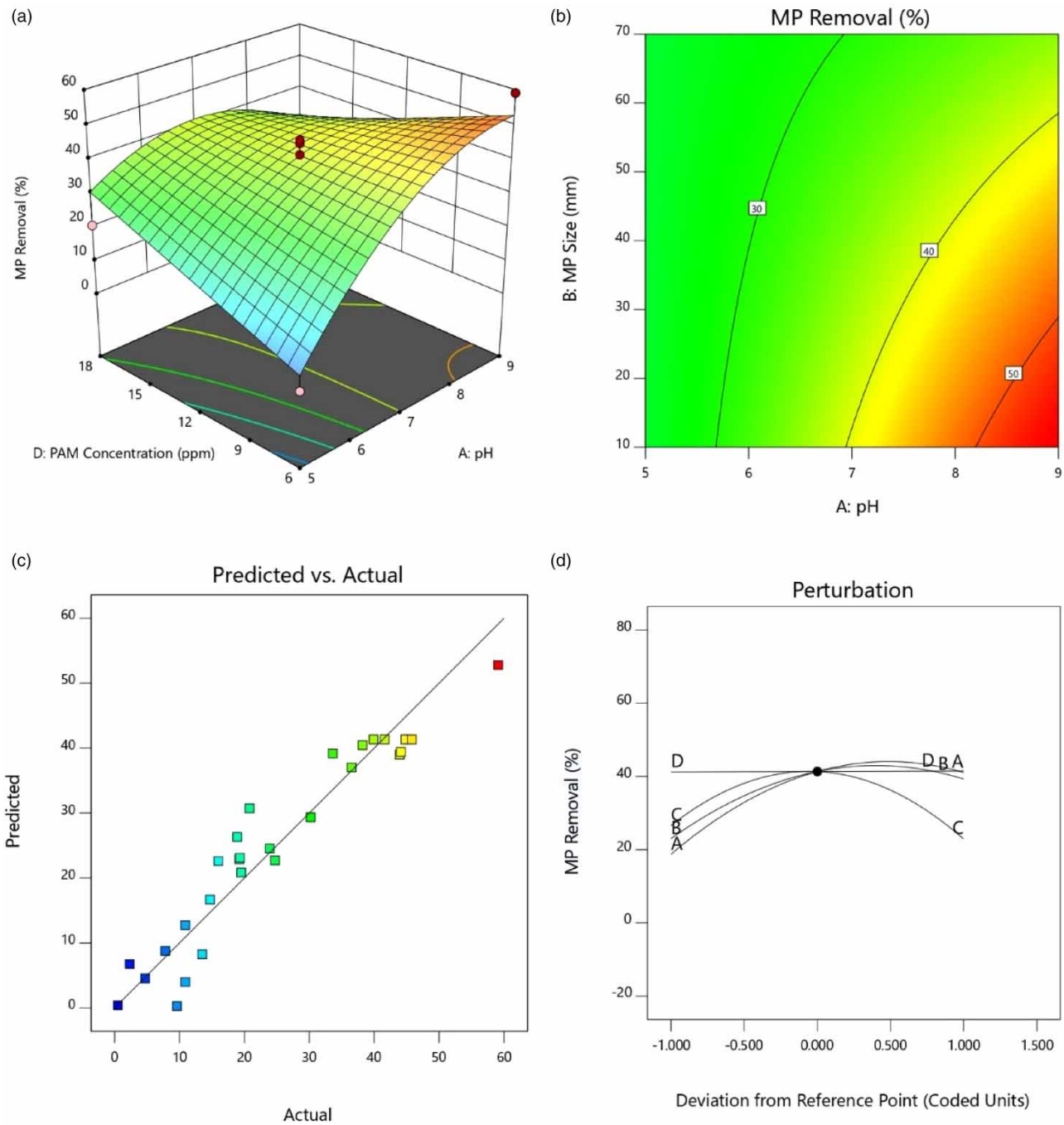

Figure 6 | Diagrams of optimum condition with PAC in which (a) shows 3-D diagram of interaction between pH and PAM concentration, (b) illustrates 2-D diagram of pH and PEMP size interaction, (c) illustrates comparison of 29 actual and predicted experiments and (d) shows perturbation plot of four analyzed variables.

range' and the response in 'Maximum' (Figure 7). The maximum predicted removal rate was chosen among 100 optimum conditions with the desirability of 0.562. Furthermore, in experiments with PAC as a coagulant, the predicted optimum condition was pH 9, PEMP size 52 μm (40–70 μm), PAC dosage of 128 ppm and PAM dosage of 6 ppm. With the mentioned conditions, the maximum removal rate of PEMPs was predicted to be 58.2%. This removal rate was also based on setting independent variables in 'In range' and the dependent variable (removal rate) in 'Maximum' and the desirability of 0.580. Finally, to test the fitness of the model with actual conditions, three experiments with PAC and three experiments with ferric chloride under the suggested conditions were conducted. In actual experiments, removal rate with PAC and ferric chloride was 51.3 ± 2.33 and 49.1 ± 2.10%, respectively. This result shows that the chosen model fairly fits the actual results. In another study, Zhang *et al.* (2021a) observed the PEMPs removal rate of 87.1% with MMHC and 92% with MMHC + Fe_3O_4 + $Mg(OH)_2$. These other coagulants that are not necessarily common can be more efficient in removing PEMPs

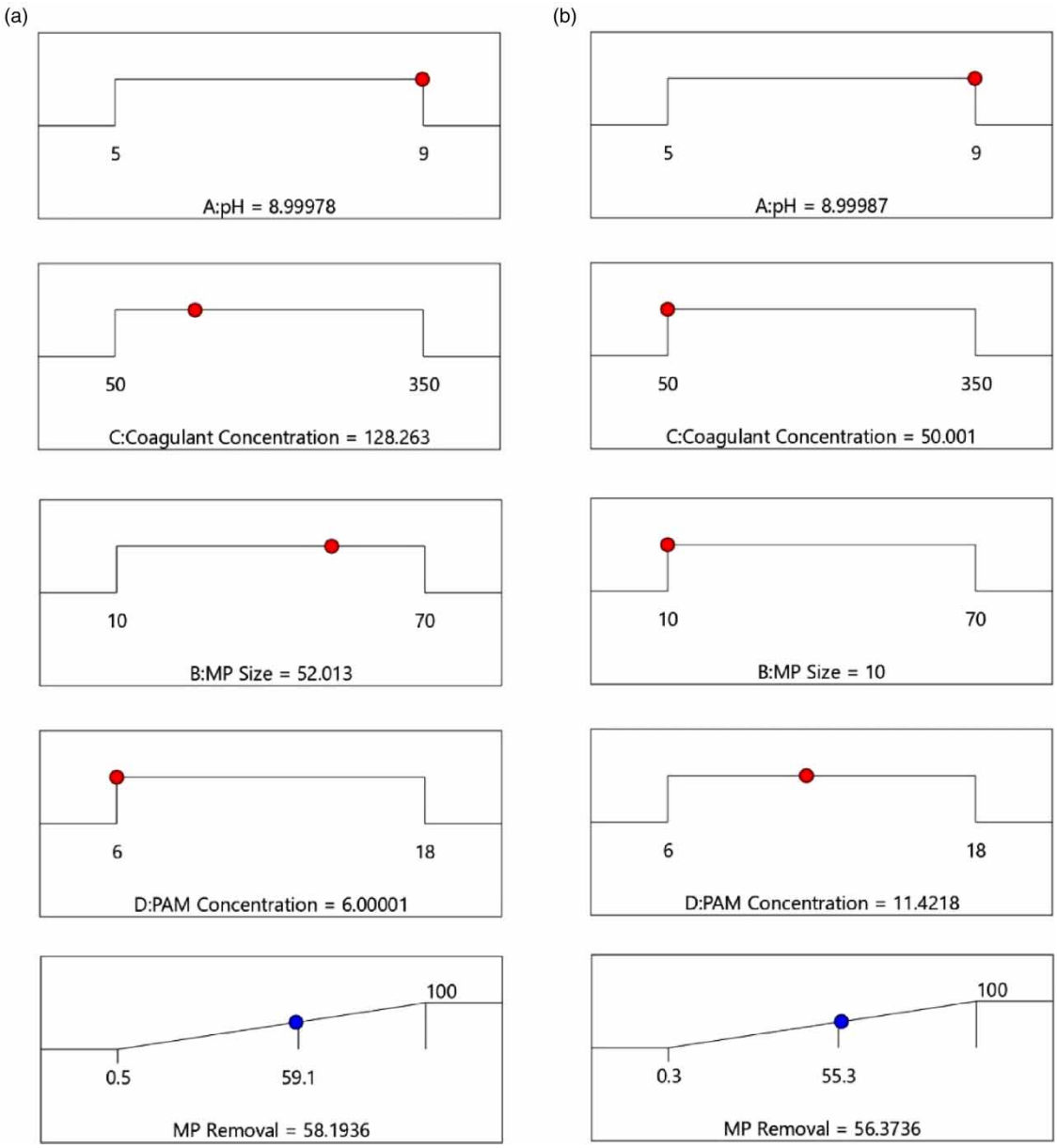

Figure 7 | Predicted optimum condition for reaching the maximum removal rate in which (a) represent the conditions with PAC as coagulant and (b) represents ferric chloride as coagulant.

(Zhang *et al.* 2021a). Moreover, Adib *et al.* (2022) in an optimized coagulation process via RSM observed the removal rate of 18.00 ± 1.43% of PPMPs with PAC as coagulant (Adib *et al.* 2022). The reason of weak removal rate can be attributed to low density of PPMPs.

Effect of disinfectants on removal rate

In this process, the effect of two common disinfectants, including O_3 and NaOCl, on removal rate of PEMPs was investigated. Common concentration of both the disinfectants used in DWTPs is between 1 and 2 ppm. In this regard, three concentrations of 1, 2 and 3 ppm were analyzed. All the experiments were conducted in suggested optimum conditions, while after 30 min of sedimentation, disinfectant was added to know if more PEMP settle. Figure 8 shows the removal rate of PEMPs with suggested concentrations of PAC or ferric chloride when 1–3 ppm O_3 or NaOCl was added.

According to Figure 8, O_3 and NaOCl had an influence on the removal rate of PEMPs after the coagulation process. One ppm of O_3 or NaOCl had a better result with ferric chloride than 2 or 3 ppm, increasing the removal rate to 58.9 and 71.5%, respectively, whereas 2 ppm of O_3 and NaOCl decreased the removal rate to 48.9 and 39.5%, respectively. On the other hand, 2 ppm of O_3 or NaOCl had a better result in removing PEMPs than 1 or 3 ppm in experiments with PAC. It has been observed that disinfecting 2 ppm of solution with O_3 or NaOCl can increase the removal rate to 76.8 and 69.1%, respectively. This difference in results with these variations in disinfectant concentration entails that more studies need to be conducted to better investigate the effect of disinfectants on MPs removal behavior. A recent study has investigated the sinking behavior of PSMPs after disinfection. Lin *et al.* (2022) observed that in O_3 treated MPs, the sinking ratio was increased to 62.3%, while chlorinated MPs decreased to a 20% sinking ratio (Lin *et al.* 2022). This difference in MPs sedimentation in contact with disinfectants can be due to degradation and mineralization of MPs surface (Li *et al.* 2022).

Further study

This study indicated that the coagulation process is not capable of removing a considerable amount of PEMPs, so other studies need to be conducted to elucidate the role of other treatment sections including granular activated carbon (GAC) or sand filtration on the removal of specific polymers of MPs. Moreover, this study showed that disinfection systems influence the removal rate. However, there usually are two steps of disinfection processes in DWTPs (primary and secondary) where the second step is right before the distribution system (Godo-Pla *et al.* 2021). Therefore, only the primary step can influence the removal rate of PEMPs in the coagulation process. Moreover, MPs are susceptible to adsorbing chemicals and undergo weathering in nature (Li *et al.* 2018; Wang *et al.* 2020a; Abdurahman *et al.* 2020; Llorca *et al.* 2020). Since this study did not control the aging of PEMPs, more studies need to be conducted to analyze the influence the rate of weathering on removal rate. According to the results of this study, PAC was a better coagulant than ferric chloride in coagulation process. Therefore, other studies are needed to analyze different types of coagulants in PEMP removal.

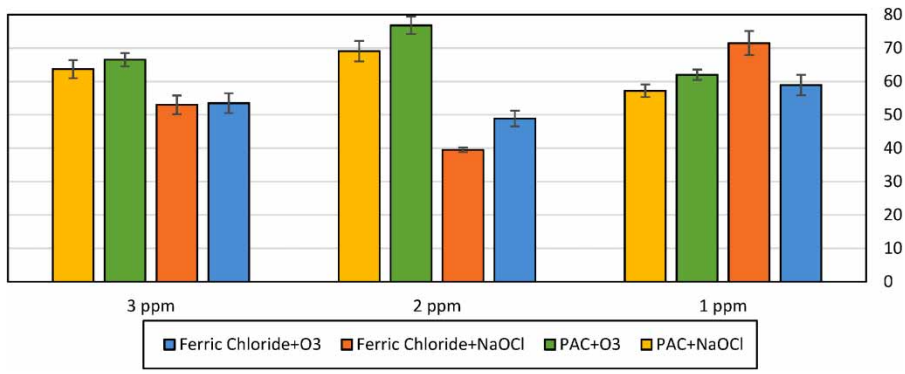

Figure 8 | Removal rate of PEMPs with suggested optimal condition and different concentrations of disinfectants. All the experiments in this section were conducted in triplicate.

CONCLUSION

This study investigated the removal characteristics of PEMPs through RSM with two commonly used coagulants and the effect of common disinfectants in PEMPs removal after coagulation. Four parameters were investigated and optimized in the coagulation process including, pH, PEMP size, coagulant and PAM concentration. In experiments with PAC as a coagulant, optimum conditions for PAM and PAC concentrations were 6 and 128 ppm, respectively, while in experiments with ferric chloride as a coagulant, the mentioned parameters were optimized at 11.4 and 50 ppm, respectively. In addition, PEMP size was optimized at 52 μm when PAC was coagulant, but when the ferric chloride was the coagulant, PEMP size was optimized at the minimum of the analyzed range. In addition, the optimum pH condition was 9 for both experiment sets with ferric chloride and PAC. According to the results, PAC was a better coagulant than ferric chloride in removing PEMPs in the coagulation process, removing 51.3 ± 2.33% in optimum conditions. Moreover, it was observed that O_3 and NaOCl as disinfectants had a significant influence on PEMPs removal after the coagulation process. Both the disinfectants increased the removal rate when PAC was coagulant in comparison with the optimum condition in the coagulation process without disinfectant (51.3 ± 2.33 and 49.1 ± 2.10% with PAC and ferric chloride, respectively).

ACKNOWLEDGEMENTS

All the expenses of this study were supported by Fatemeh Tabatabaei. We are grateful to the Islamic Azad University, West Tehran Branch for providing equipment to conduct this study.

DATA AVAILABILITY STATEMENT

All relevant data are included in the paper or its Supplementary Information.

CONFLICT OF INTEREST

The authors declare there is no conflict.

REFERENCES

Abdurahman, A., Cui, K., Wu, J., Li, S., Gao, R., Dai, J., Liang, W. & Zeng, F. 2020 Adsorption of dissolved organic matter (DOM) on polystyrene microplastics in aquatic environments: kinetic, isotherm and site energy distribution analysis. *Ecotoxicology and Environmental Safety* **198**, 110658.

Adib, D., Mafigholami, R. & Tabeshkia, H. 2021 Identification of microplastics in conventional drinking water treatment plants in Tehran, Iran. *Journal of Environmental Health Science and Engineering* **19** (2), 1817–1826.

Adib, D., Mafigholami, R., Tabeshkia, H. & Walker, T. R. 2022 Optimization of polypropylene microplastics removal using conventional coagulants in drinking water treatment plants via response surface methodology. *Journal of Environmental Health Science and Engineering* **20**, 565–577.

Ahmad, A. L., Wong, S. S., Teng, T. T. & Zuhairi, A. 2008 Improvement of alum and PACl coagulation by polyacrylamides (PAMs) for the treatment of pulp and paper mill wastewater. *Chemical Engineering Journal* **137** (3), 510–517.

Anderson, P. J., Warrack, S., Langen, V., Challis, J. K., Hanson, M. L. & Rennie, M. D. 2017 Microplastic contamination in Lake Winnipeg, Canada. *Environmental Pollution* **225**, 223–231.

Çobanoğlu, H., Belivermiş, M., Sıkdokur, E., Kılıç, Ö. & Çayır, A. 2021 Genotoxic and cytotoxic effects of polyethylene microplastics on human peripheral blood lymphocytes. *Chemosphere* **272**, 129805.

Crew, A., Gregory-Eaves, I. & Ricciardi, A. 2020 Distribution, abundance, and diversity of microplastics in the upper St. Lawrence River. *Environmental Pollution* **260**, 113994.

Esfandiari, A. & Mowla, D. 2021 Investigation of microplastic removal from greywater by coagulation and dissolved air flotation. *Process Safety and Environmental Protection* **151**, 341–354.

Godo-Pla, L., Rodríguez, J. J., Suquet, J., Emiliano, P., Valero, F., Poch, M. & Monclús, H. 2021 Control of primary disinfection in a drinking water treatment plant based on a fuzzy inference system. *Process Safety and Environmental Protection* **145**, 63–70.

Grbić, J., Helm, P., Athey, S. & Rochman, C. M. 2020 Microplastics entering northwestern Lake Ontario are diverse and linked to urban sources. *Water Research* **174**, 115623.

Hashempour, Y. & Mortezazadeh, F. 2020 Changes in water quality parameters in different processes of surface water treatment plant (Case study: Tehranpars water treatment plant). *Journal of Mazandaran University of Medical Sciences* **30** (189), 107–116.

Hebner, T. S. & Maurer-Jones, M. A. 2020 Characterizing microplastic size and morphology of photodegraded polymers placed in simulated moving water conditions. *Environmental Science: Processes & Impacts* **22** (2), 398–407.

Hwang, J., Choi, D., Han, S., Jung, S. Y., Choi, J. & Hong, J. 2020 Potential toxicity of polystyrene microplastic particles. *Scientific Reports* **10** (1), 7391.

Jaikumar, G., Brun, N. R., Vijver, M. G. & Bosker, T. 2019 Reproductive toxicity of primary and secondary microplastics to three cladocerans during chronic exposure. *Environmental Pollution* **249**, 638–646.

Jiang, J.-Q. 2015 The role of coagulation in water treatment. *Current Opinion in Chemical Engineering* **8**, 36–44.

Kay, P., Hiscoe, R., Moberley, I., Bajic, L. & McKenna, N. 2018 Wastewater treatment plants as a source of microplastics in river catchments. *Environmental Science and Pollution Research* **25** (20), 20264–20267.

Kelkar, V. P., Rolsky, C. B., Pant, A., Green, M. D., Tongay, S. & Halden, R. U. 2019 Chemical and physical changes of microplastics during sterilization by chlorination. *Water Research* **163**, 114871.

Kim, S.-C. 2016 Application of response surface method as an experimental design to optimize coagulation–flocculation process for pre-treating paper wastewater. *Journal of Industrial and Engineering Chemistry* **38**, 93–102.

Klein, M. & Fischer, E. K. 2019 Microplastic abundance in atmospheric deposition within the Metropolitan area of Hamburg, Germany. *Science of The Total Environment* **685**, 96–103.

Li, J., Zhang, K. & Zhang, H. 2018 Adsorption of antibiotics on microplastics. *Environmental Pollution* **237**, 460–467.

Li, C., Busquets, R., Moruzzi, R. B. & Campos, L. C. 2021 Preliminary study on low-density polystyrene microplastics bead removal from drinking water by coagulation-flocculation and sedimentation. *Journal of Water Process Engineering* **44**, 102346.

Li, Y., Li, J., Ding, J., Song, Z., Yang, B., Zhang, C. & Guan, B. 2022 Degradation of nano-sized polystyrene plastics by ozonation or chlorination in drinking water disinfection processes. *Chemical Engineering Journal* **427**, 131690.

Lin, L., Zuo, L.-Z., Peng, J.-P., Cai, L.-Q., Fok, L., Yan, Y., Li, H.-X. & Xu, X.-R. 2018 Occurrence and distribution of microplastics in an urban river: a case study in the Pearl River along Guangzhou City, China. *Science of The Total Environment* **644**, 375–381.

Lin, J., Wu, X., Liu, Y., Fu, J., Chen, Y. & Ou, H. 2022 Sinking behavior of polystyrene microplastics after disinfection. *Chemical Engineering Journal* **427**, 130908.

Liu, T., Lian, Y., Graham, N., Yu, W., Rooney, D. & Sun, K. 2017 Application of polyacrylamide flocculation with and without alum coagulation for mitigating ultrafiltration membrane fouling: role of floc structure and bacterial activity. *Chemical Engineering Journal* **307**, 41–48.

Llorca, M., Ábalos, M., Vega-Herrera, A., Adrados, M. A., Abad, E. & Farré, M. 2020 Adsorption and desorption behaviour of polychlorinated biphenyls onto microplastics' surfaces in water/sediment systems. *Toxics* **8** (3), 59.

Lu, S., Liu, L., Yang, Q., Demissie, H., Jiao, R., An, G. & Wang, D. 2021 Removal characteristics and mechanism of microplastics and tetracycline composite pollutants by coagulation process. *Science of The Total Environment* **786**, 147508.

Ma, B., Xue, W., Ding, Y., Hu, C., Liu, H. & Qu, J. 2019a Removal characteristics of microplastics by Fe-based coagulants during drinking water treatment. *Journal of Environmental Science (China)* **78**, 267–275.

Ma, B., Xue, W., Hu, C., Liu, H., Qu, J. & Li, L. 2019b Characteristics of microplastic removal via coagulation and ultrafiltration during drinking water treatment. *Chemical Engineering Journal* **359**, 159–167.

Magni, S., Binelli, A., Pittura, L., Avio, C. G., Della Torre, C., Parenti, C. C., Gorbi, S. & Regoli, F. 2019 The fate of microplastics in an Italian Wastewater Treatment Plant. *Science of The Total Environment* **652**, 602–610.

Mao, R., Hu, Y., Zhang, S., Wu, R. & Guo, X. 2020a Microplastics in the surface water of Wuliangsuhai Lake, northern China. *Science of The Total Environment* **723**, 137820.

Mao, R., Lang, M., Yu, X., Wu, R., Yang, X. & Guo, X. 2020b Aging mechanism of microplastics with UV irradiation and its effects on the adsorption of heavy metals. *Journal of Hazardous Materials* **393**, 122515.

Monira, S., Bhuiyan, M. A., Haque, N. & Pramanik, B. K. 2021 Assess the performance of chemical coagulation process for microplastics removal from stormwater. *Process Safety and Environmental Protection* **155**, 11–16.

Nakazawa, Y., Abe, T., Matsui, Y., Shinno, K., Kobayashi, S., Shirasaki, N. & Matsushita, T. 2021 Differences in removal rates of virgin/decayed microplastics, viruses, activated carbon, and kaolin/montmorillonite clay particles by coagulation, flocculation, sedimentation, and rapid sand filtration during water treatment. *Water Research* **203**, 117550.

Paço, A., Duarte, K., da Costa, J. P., Santos, P. S. M., Pereira, R., Pereira, M. E., Freitas, A. C., Duarte, A. C. & Rocha-Santos, T. A. P. 2017 Biodegradation of polyethylene microplastics by the marine fungus Zalerion maritimum. *Science of The Total Environment* **586**, 10–15.

Parsa, M. M., Pourfakhar, H. & Baghdadi, M. 2020 Application of graphene oxide nanosheets in the coagulation-flocculation process for removal of Total Organic Carbon (TOC) from surface water. *Journal of Water Process Engineering* **37**, 101367.

Pivokonsky, M., Cermakova, L., Novotna, K., Peer, P., Cajthaml, T. & Janda, V. 2018 Occurrence of microplastics in raw and treated drinking water. *Science of The Total Environment* **643**, 1644–1651.

Pivokonský, M., Pivokonská, L., Novotná, K., Čermáková, L. & Klimtová, M. 2020 Occurrence and fate of microplastics at two different drinking water treatment plants within a river catchment. *Science of The Total Environment* **741**, 140236.

PlasticEurope 2021 Plastics – the Facts 2021. An analysis of European plastics production, demand and waste data. the Association of Plastics Manufacturers in Europe, p. 34.

Prata, J. C. 2018 Microplastics in wastewater: state of the knowledge on sources, fate and solutions. *Marine Pollution Bulletin* **129** (1), 262–265.

Qiang, L. & Cheng, J. 2021 Exposure to polystyrene microplastics impairs gonads of zebrafish (Danio rerio). *Chemosphere* **263**, 128161.

Raju, S., Carbery, M., Kuttykattil, A., Senathirajah, K., Subashchandrabose, S. R., Evans, G. & Thavamani, P. 2018 Transport and fate of microplastics in wastewater treatment plants: implications to environmental health. *Reviews in Environmental Science and Bio/Technology* **17** (4), 637–653.

Rawi, S., Nenov, V., Aidan, A. & Essawi, E. 2014 Optimization of coagulation process in high turbidity discharged from ceramic factories. *International J.of Multidispl.Research & Advcs. in Engg.(IJMRAE)* **6** (4), 69–80.

Sarmah, P. & Rout, J. 2018 Efficient biodegradation of low-density polyethylene by cyanobacteria isolated from submerged polyethylene surface in domestic sewage water. *Environmental Science and Pollution Research* **25** (33), 33508–33520.

Schmidt, C., Kumar, R., Yang, S. & Büttner, O. 2020 Microplastic particle emission from wastewater treatment plant effluents into river networks in Germany: loads, spatial patterns of concentrations and potential toxicity. *Science of The Total Environment* **737**, 139544.

Selvamani, V., 2019 Chapter 15 - Stability studies on nanomaterials used in drugs. In: *Characterization and Biology of Nanomaterials for Drug Delivery* (Mohapatra, S. S., Ranjan, S., Dasgupta, N., Mishra, R. K. & Thomas, S., eds). Elsevier, Amsterdam, pp. 425–444.

Shruti, V. C., Pérez-Guevara, F. & Kutralam-Muniasamy, G. 2020 Metro station free drinking water fountain- A potential 'microplastics hotspot' for human consumption. *Environ Pollut* **261**, 114227.

Sighicelli, M., Pietrelli, L., Lecce, F., Iannilli, V., Falconieri, M., Coscia, L., Di Vito, S., Nuglio, S. & Zampetti, G. 2018 Microplastic pollution in the surface waters of Italian Subalpine Lakes. *Environmental Pollution* **236**, 645–651.

Sillanpää, M., Ncibi, M. C., Matilainen, A. & Vepsäläinen, M. 2018 Removal of natural organic matter in drinking water treatment by coagulation: a comprehensive review. *Chemosphere* **190**, 54–71.

Singh, B. & Kumar, P. 2020 Pre-treatment of petroleum refinery wastewater by coagulation and flocculation using mixed coagulant: optimization of process parameters using response surface methodology (RSM). *Journal of Water Process Engineering* **36**, 101317.

Tang, K. H. D. & Hadibarata, T. 2021 Microplastics removal through water treatment plants: its feasibility, efficiency, future prospects and enhancement by proper waste management. *Environmental Challenges* **5**, 100264.

Tong, H., Jiang, Q., Hu, X. & Zhong, X. 2020 Occurrence and identification of microplastics in tap water from China. *Chemosphere* **252**, 126493.

Wang, H. T., Ye, Y. Y., Qi, J., Li, F. T. & Tang, Y. L. 2013 Removal of titanium dioxide nanoparticles by coagulation: effects of coagulants, typical ions, alkalinity and natural organic matters. *Water Science and Technology* **68** (5), 1137–1143.

Wang, Q., Zhang, Y., Wangjin, X., Wang, Y., Meng, G. & Chen, Y. 2020a The adsorption behavior of metals in aqueous solution by microplastics effected by UV radiation. *Journal of Environmental Sciences* **87**, 272–280.

Wang, Z., Lin, T. & Chen, W. 2020b Occurrence and removal of microplastics in an advanced drinking water treatment plant (ADWTP). *Science of The Total Environment* **700**, 134520.

Wright, S. L., Ulke, J., Font, A., Chan, K. L. A. & Kelly, F. J. 2020 Atmospheric microplastic deposition in an urban environment and an evaluation of transport. *Environment International* **136**, 105411.

Wu, W.-M., Yang, J. & Criddle, C. S. 2016 Microplastics pollution and reduction strategies. *Frontiers of Environmental Science & Engineering* **11** (1), 6.

Xiong, B., Loss, R. D., Shields, D., Pawlik, T., Hochreiter, R., Zydney, A. L. & Kumar, M. 2018 Polyacrylamide degradation and its implications in environmental systems. *npj Clean Water* **1** (1), 17.

Xue, J., Peldszus, S., Van Dyke, M. I. & Huck, P. M. 2021 Removal of polystyrene microplastic spheres by alum-based coagulation-flocculation-sedimentation (CFS) treatment of surface waters. *Chemical Engineering Journal* **422**, 130023.

You, H., Huang, B., Cao, C., Liu, X., Sun, X., Xiao, L., Qiu, J., Luo, Y., Qian, Q. & Chen, Q. 2021 Adsorption–desorption behavior of methylene blue onto aged polyethylene microplastics in aqueous environments. *Marine Pollution Bulletin* **167**, 112287.

Zhang, Y., Zhao, J., Liu, Z., Tian, S., Lu, J., Mu, R. & Yuan, H. 2021a Coagulation removal of microplastics from wastewater by magnetic magnesium hydroxide and PAM. *Journal of Water Process Engineering* **43**, 102250.

Zhang, Y., Zhou, G., Yue, J., Xing, X., Yang, Z., Wang, X., Wang, Q. & Zhang, J. 2021b Enhanced removal of polyethylene terephthalate microplastics through polyaluminum chloride coagulation with three typical coagulant aids. *Science of The Total Environment* **800**, 149589.

Zhang, Y., Wang, S., Olga, V., Xue, Y., Lv, S., Diao, X., Zhang, Y., Han, Q. & Zhou, H. 2022 The potential effects of microplastic pollution on human digestive tract cells. *Chemosphere* **291**, 132714.

Zhou, Y., Yang, Y., Liu, G., He, G. & Liu, W. 2020 Adsorption mechanism of cadmium on microplastics and their desorption behavior in sediment and gut environments: the roles of water pH, lead ions, natural organic matter and phenanthrene. *Water Research* **184**, 116209.

Zhou, G., Wang, Q., Li, J., Li, Q., Xu, H., Ye, Q., Wang, Y., Shu, S. & Zhang, J. 2021 Removal of polystyrene and polyethylene microplastics using PAC and fecl3 coagulation: performance and mechanism. *Science of The Total Environment* **752**, 141837.

First received 24 July 2022; accepted in revised form 21 November 2022. Available online 28 November 2022